Fatty acid metabolism in adipocytes: functional analysis of fatty acid transport proteins 1 and 4

Sandra Lobo, Brian M. Wiczer, Ann J. Smith, Angela M. Hall, and David A. Bernlohr[1]

Department of Biochemistry, Molecular Biology, and Biophysics, University of Minnesota, Minneapolis, MN 55455

Abstract   The role of fatty acid transport protein 1 (FATP1) and FATP4 in facilitating adipocyte fatty acid metabolism was investigated using stable FATP1 or FATP4 knockdown (kd) 3T3-L1 cell lines derived from retrovirus-delivered short hairpin RNA (shRNA). Decreased expression of FATP1 or FATP4 did not affect preadipocyte differentiation or the expression of FATP1 (in FATP4 kd), FATP4 (in FATP1 kd), fatty acid translocase, acyl-coenzyme A synthetase 1, and adipocyte fatty acid binding protein but did lead to increased levels of peroxisome proliferator-activated receptor γ and CCAAT/enhancer binding protein α. Both FATP1 and FATP4 kd adipocytes exhibited reduced triacylglycerol deposition and corresponding reductions in diacylglycerol and monoacylglycerol levels compared with control cells. FATP1 kd adipocytes displayed an ~25% reduction in basal ^{3}H-labeled fatty acid uptake and a complete loss of insulin-stimulated ^{3}H-labeled fatty acid uptake compared with control adipocytes. In contrast, FATP4 kd adipocytes as well as HEK-293 cells overexpressing FATP4 did not display any changes in fatty acid influx. FATP4 kd cells exhibited increased basal lipolysis, whereas FATP1 kd cells exhibited no change in lipolytic capacity. Consistent with reduced triacylglycerol accumulation, FATP1 and FATP4 kd adipocytes exhibited enhanced 2-deoxyglucose uptake compared with control adipocytes.▪ These findings define unique and distinct roles for FATP1 and FATP4 in adipose fatty acid metabolism.—Lobo, S., B. M. Wiczer, A. J. Smith, A. M. Hall, and D. A. Bernlohr. **Fatty acid metabolism in adipocytes: functional analysis of fatty acid transport proteins 1 and 4.** *J. Lipid Res.* 2007. **48:** 609–620.

Dysregulation in adipose fatty acid metabolism is a significant contributing factor to the development of obesity and associated metabolic diseases, such as type 2 diabetes, hypertension, and cardiovascular disease (1–3). Central to this imbalance are differing rates of long-chain fatty acid (LCFA) influx, efflux, and metabolism by adipose tissue. Although appreciated for decades, the molecular mechanisms that control and mediate fatty acid flux in fat cells remain poorly defined from structural, mechanistic, and regulatory viewpoints.

Although diffusion may play a fundamental role in the transbilayer movement of LCFA, molecular and genetic evidence from loss- or gain-of-function studies have identified a number of proteins facilitating some component of the fatty acid influx process (4–8). Proteins implicated in fatty acid uptake are fatty acid translocase (CD36), acyl-CoA synthetases [fatty acid transport protein (FATP) and acyl-coenzyme A synthetase (ACSL) family members], plasma membrane fatty acid binding protein, and caveolin-1. The relative contribution of each polypeptide to overall cellular fatty acid influx has not been quantitatively evaluated.

FATPs are a family of membrane-bound proteins that catalyze the ATP-dependent esterificaton of LCFAs and very LCFAs to their acyl-CoA derivatives (9). The FATPs bear 20–40% sequence identity to the long-chain ACSL class of proteins that function in long-chain acyl-CoA production. In mammals, six different isoforms of FATP (FATP1 to FATP6) have been identified with tissue-specific expression patterns (10). White adipose tissue predominantly expresses FATP1, FATP4, and ACSL1, whereas brown adipose tissue additionally expresses ACSL5.

FATP1 is a 63 kDa protein localized primarily to high-density membranes and to a lesser extent in the plasma and low-density membrane fractions of murine adipocytes and 3T3-L1 cells (5). FATP1 (as well as ACSL1) was identified using an expression clone strategy designed to identify proteins that enhanced LCFA uptake (11). Evidence for the role of FATPs in fatty acid transport has been qualitatively evaluated by various loss-of-function/gain-of-function model systems. Stable HEK-293 cell lines over-

expressing murine FATP1 demonstrate increased LCFA uptake and triacylglycerol accumulation (12). A transgenic mouse model with cardiac-specific expression of FATP1 demonstrated increased myocardial LCFA uptake (13). Disruption of the FATP1 homolog expressed in yeast, fat1p, markedly impaired LCFA uptake (14), and a murine FATP1 knockout mouse exhibited reduced muscle acyl-CoA levels and increased insulin sensitivity (15).

FATP4 is the closest homolog of FATP1 (60.3% identity) that is expressed in adipose tissue (16). It role in adipose tissue metabolism is largely unknown. However, FATP4 is also expressed in skeletal muscle, heart, skin, and liver and is the principal fatty acid transporter in the small intestine, localized to the apical side of enterocytes, where it is thought to mediate the uptake of dietary fatty acids (17). *FATP4* null mice displayed features of a human neonatally lethal restrictive dermopathy that has been associated with a disturbed function in the epidermal barrier (18–20). FATP4 encodes an ACSL with substrate specificity to very LCFAs that may be required for the synthesis of lipids crucial in the formation of a healthy epidermis (21, 22). Polymorphisms in the human *FATP4* gene locus have identified this gene as a candidate for the insulin resistance syndrome (23). Moreover, FATP4 expression levels correlated with measures of acquired obesity and insulin resistance (24). These observations indicate the importance of the study of FATP4 function in adipocyte fatty acid uptake and metabolism.

Our long-term goal is to identify and define in quantitative terms the mechanisms controlling LCFA flux in mammalian cells and the roles of specific proteins implicated in the influx reaction. In this report, we evaluated the specific role(s) of FATP1 and FATP4 in mediating LCFA influx and efflux using FATP1/FATP4 knockdown (FATP1/FATP4 kd) 3T3-L1 adipocytes produced using lentiviral delivery of short hairpin RNA (shRNA) targeted toward FATP1 or FATP4. We report here that FATP1 facilitates the insulin-stimulated component of LCFA uptake but has only a minor role in basal LCFA uptake in 3T3-L1 adipocytes. FATP4 does not play a rate-limiting role in either basal or insulin-stimulated fatty acid uptake. FATP4 kd adipocytes exhibited increased basal lipolysis, suggesting a role in fatty acid reesterification in 3T3-L1 adipocytes.

MATERIALS AND METHODS

Materials

Cell culture reagents were obtained from Invitrogen. Porcine insulin, puromycin, cytocholasin B, and deoxyglucose were obtained from Sigma-Aldrich. Geneticin was obtained from Gibco/BRL Life Technologies. Nonradiolabeled fatty acids were obtained from Nu-Chek Prep, Inc. (Elysian, MN). [³H]oleic acid and [³H]lignoceric acid were obtained from American Radiochemicals Co. [³H]palmitic acid, [³H]arachidonic acid, and [¹⁴C]2-deoxy-D-glucose were obtained from Amersham Pharmacia Biotech.

Antibodies used were as follows: rabbit anti-CD36, rabbit anti-peroxisome proliferator-activated receptor γ (PPARγ), and rabbit anti-CCAAT/enhancer binding protein α (C/EBPα; obtained from Santa Cruz Biotechnology, Inc.); rabbit anti-GLUT4 (a gift from Dr. H. Haspel, Charles River Laboratory, Wilmington, MA); rabbit anti-ACSL1 (a gift from Dr. Rosalind Coleman, University of North Carolina, Chapel Hill, NC); rabbit anti-FATP4 (a gift from Dr. Paul Watkins, Kennedy Krieger Research Institute, Baltimore, MD); and HRP-coupled IgGs (obtained from Jackson ImmunoResearch Laboratories, Inc.). All other reagents were of analytical grade and obtained from Sigma.

Cell culture conditions

3T3-L1 preadipocytes were cultured and differentiated into adipocytes as described previously (25). Briefly, preadipocytes were cultured in DMEM containing 10% calf serum. Two days after reaching confluence, cells were induced to differentiate in DMEM supplemented with 10% FBS, 174 μM insulin, 0.5 mM methylisobutylxanthine, and 0.25 μM dexamethasone. Two days after initiation of differentiation, dexamethasone and methylisobutylxanthine were withdrawn from the medium, whereas insulin was withdrawn after 4 days. Differentiated adipocytes were maintained in DMEM and 10% FBS until mature (days 8–12).

Generation of FATP1 kd and FATP4 kd 3T3-L1 adipocytes using lentivirus-delivered RNA interference

The lentivirus-based RNA interference (RNAi) vector pLKO1 (kindly provided by Sheila Stewart at the Whitehead Institute, Cambridge, MA) was used for siRNA-mediated FATP1 kd in cultured 3T3-L1 cells. This vector was shown to stably expresses shRNAs under the control of the RNA polymerase III promoter of the U6 gene in nondividing cells (26). Oligomers 60 bp in length containing a stem-loop structure directed against FATP1 and FATP4 were synthesized and cloned into the *Age*I/*Eco*RI site in pLKO1. Four siRNA sequence variants for each gene were synthesized and analyzed. Based on the ability of the lentiviral RNAi vector to effectively silence the expression of FATP1/FATP4 by 75% or more in HEK-293T cells transiently cotransfected with a FATP1/FATP4 expression vector and each of the four lentiviral RNAi vectors, one of the gene sequence variant constructs was selected for the generation of recombinant lentiviruses. The selected oligomer targeting the FATP1 nucleotide sequence was 5′-TGCTGTAGCCAACCTGTTCC-3′ (nucleotide positions 342–361) and that targeting the FATP4 nucleotide sequence was 5′-GGCACGAGCTCTCATCTT-3′ (nucleotide positions 519–536). A construct expressing shRNA against a scrambled FATP1 sequence (5′-TAGGTCTTCAAGAGGGGATG-3′) was used as a control. Recombinant lentiviruses were packaged in HEK-293T cells and harvested at 24, 48, and 72 h later (4). 3T3-L1 fibroblasts were transduced with the lentiviruses for 4–6 h in the presence of 6 μg/ml polybrene at a multiplicity of infection of ∼50–100. Cells were allowed to recover for 48 h after transduction before the addition of selection media containing 2 μg/ml puromycin. Stable kd cell lines were generated from a heterogeneous pool of puromycin-resistant 3T3-L1 fibroblasts.

Generation of stable HEK-293 cells expressing FATP4

FATP4 subcloned into pcDNA3.0 (Invitrogen) or vector control was linearized and introduced into HEK-293 cells by electroporation. HEK-293 cells are an excellent model system to evaluate FATP4 function in lipid metabolism because they are a well-defined cell system, grow easily in culture, and have been shown to tolerate FATP expression (12). Dilutions of the electroporated cells were plated in DMEM containing 10% FBS and incubated at 37°C and 5% CO_2. Selection was initiated after 48 h with the addition of 400 μg/ml geneticin. After 8 days, colonies were selected using cloning rings and individual lines were developed. Once established, several lines were analyzed for FATP4

expression. The cell lines and vector control cells were maintained in 400 μg/ml geneticin. FATP4-overexpressing cell lines were analyzed for total cellular lignoceryl (C24:0) CoA synthetase activities and oleate (C18:1) uptake by a procedure similar to that used for 3T3-L1 adipocytes.

Immunoblot analysis

3T3-L1 adipocytes were lysed in a buffer containing 50 mM Tris-HCl, pH 7.5, 50 mM sodium fluoride, 5 mM sodium pyrophosphate, 1 mM ethylenediamine tetraacetic acid, 1 mM dithiothreitol, 0.1 mM phenylmethyl sulfonyl fluoride, 10% glycerol, and protease and phosphatase inhibitors. Crude cell extracts (50–100 μg of total protein) were separated by electrophoresis on a denaturing SDS-polyacrylamide gel and transferred to nitrocellulose or polyvinylidene difluoride membranes. The membranes were blocked with 5% nonfat milk in TBST (100 mM Tris, pH 7.4, 0.9% sodium chloride, and 0.05% Tween-20) for 1 h at room temperature. After incubation with primary antibodies, the membranes were incubated with secondary antibodies conjugated to horseradish peroxidase. Antibody reactivity was detected by chemiluminescence, and protein abundance was quantitated by densitometry using a FujiFilm FLA-5000 detector.

Analysis of cellular fatty acid uptake

3T3-L1 adipocytes (day 8) were preincubated for 3 h in Krebs-Ringer's HEPES (KRH) buffer (pH 7.4) containing 120 mM NaCl, 4.7 mM KCl, 2.2 mM CaCl$_2$, 10 mM HEPES, 1.2 mM KH$_2$PO$_4$, 1.2 mM MgSO$_4$, and 5.4 mM glucose. Stock solutions (5 mM) of nonradioactive fatty acids were prepared. Radioactive ^{3}H-labeled fatty acids (1 mCi/mmol) were added to achieve the final specific activity. Adipocytes were incubated either with or without insulin (50–100 nM) for 30 min, and fatty acid uptake was initiated by incubating cells in KRH buffer, pH 7.4, containing 5.4 mM glucose and 50 μM [^{3}H]palmitic, oleic, or arachidonic acid, each bound to fatty acid-free BSA in a ratio adjusted to generate a free fatty acid concentration of 5 nM. The appropriate FA/BSA ratios for the different fatty acids used in the assay were calculated using LCFA binding constants for BSA as described by Richieri, Anel, and Kleinfeld (27). After 5 min, the cells were rapidly washed three times in ice-cold KRH containing 0.1% BSA and 200 μM phloretin. The cells were then incubated at room temperature in 0.5% SDS for 30 min, and the cell-incorporated radioactive fatty acids were determined by liquid scintillation counting.

Lipid analysis

After cellular influx of radioactive fatty acids, fatty acyl-CoAs were extracted using Dole's reagent. The organic phase was dried down, taken up in a minimal volume of chloroform, and bound to disposable primary aminopropyl bonded phase columns. The various polar and neutral classes of lipids were eluted off the column by organic fractionation using the procedures outlined by Kaluzny et al. (28) and quantitated by liquid scintillation counting. Cellular triacylglycerol, diacylglycerol, and monoacylglycerol lipids fractionated by the procedure described above were quantitated by alkaline hydrolysis and measurement of glycerol content using the glycerol determination kit (Sigma). Fatty acids were measured using a NEFA kit (Wako).

Fatty ACSL assays

Cells were harvested in 150 mM Tris-HCl, 150 mM NaCl, and 250 mM sucrose, pH 7.5, and lysed via sonication immediately before assaying activity. Extracts were assayed for ACSL activity by the conversion of [^{3}H]palmitic acid, [^{3}H]oleic acid, [^{3}H]arachi-

donic acid, or [^{3}H]lignoceric acid to their CoA derivatives by a modified method from Nagamatsu et al. (29) as described by Hall, Smith, and Bernlohr (9). Briefly, samples were assayed for 2 min at pH 7.5 and 30 mM NaCl in 250 μl of a buffer containing 20 μM fatty acid delivered bound to α-cyclodextrin, 100 mM Tris-HCl (pH 7.5), 10 mM ATP, 5 mM MgCl$_2$, 200 μM CoA, and 200 μM dithiothreitol. Reactions were terminated with the addition of 1.25 ml of isopropanol/heptane/H$_2$SO$_4$ (40:10:1, v/v/v), 0.5 ml of water, and 0.75 ml of heptane to facilitate organic phase separation. The aqueous phase was extracted three times with 0.75 ml of heptane to remove unreacted fatty acids, and the radioactivity was determined by liquid phase scintillation counting.

Immunoflorescence analysis of 3T3-L1 adipocytes

3T3-L1 cells were plated on 13 mm optical glass coverslips and differentiated as described previously. On day 6, the cells were washed free of serum and maintained in DMEM for 2 h. Insulin was added (50 ng/ml), and after 30 min the cells were washed in PBS and fixed in 3% paraformaldehyde for 30 min at 25°C. After fixation, the cells were rinsed in PBS containing 0.01% digitonin and incubated for 2 h at 25°C in blocking buffer containing 0.01 M phosphate, 5% goat serum, 5% glycerol, 1.0% cold water fish gelatin, and 0.01% digitonin. The cells were subsequently incubated overnight at 4°C in a 1:50 dilution of rabbit anti-FATP1 or anti-FATP4 antibody or in a 1:100 dilution of rabbit anti-GLUT4 antibody in PBS containing 0.01% digitonin. After washing, the coverslips were incubated for 1 h at 25°C in a 1:400 dilution of Alexa Fluor 488-conjugated donkey anti-rabbit IgG in PBS with 0.01% digitonin. After washing, the coverslips were incubated at 25°C in DMEM with 7.7 μM TOPRO3 (Molecular Probes) for nuclear staining, then washed, mounted, and visualized by confocal microscopy.

Confocal microscopy

Monolayers were viewed using a Bio-Rad MRC-1024 confocal microscope attached to a Nikon Diaphot inverted microscope equipped with a 15 mW krypton/argon laser. Excitation filters allowing 488 and 647 nm were used sequentially to visualize the Alexa Fluor 488 and TOPRO3 probes, respectively. Digital images were collected using LaserSharp version 3.2 software (Bio-Rad) and analyzed using Image Pro Plus version 4.5 software (Media Cybernetics, Silver Spring, MD).

Analysis of 2-deoxyglucose uptake

Glucose uptake in 3T3-L1 adipocytes was carried out as described (30). Briefly, cells were serum-starved in KRH buffer supplemented with 0.5% BSA and 2 mM sodium pyruvate (pH 7.4) and incubated either with or without 100 nM insulin for 30 min at 37°C. Glucose uptake was initiated by the addition of [^{14}C]2-deoxy-D-glucose to a final assay concentration of 100 μM at 37°C. After 5 min, 2-deoxyglucose uptake was terminated by three washes with ice-cold KRH buffer, and the cells were solubilized with 0.8 ml of KRH buffer containing 1% Triton X-100. The incorporated radioactivity was determined by scintillation counting. Nonspecific 2-deoxyglucose uptake was measured in the presence of 20 μM cytocholasin B and subtracted from the total glucose uptake assayed to determine specific uptake.

RESULTS

To assess the role of FATP1 and FATP4 in fatty acid metabolism in adipocytes, we used stable 3T3-L1 adipocyte

FATP1 kd and FATP4 kd cell lines derived from lentivirus-delivered shRNA targeting either protein. Such kd pre-adipocytes grew at a normal rate and differentiated using the standard methylisobutylxanthine, dexamethasone, and insulin protocol. An essentially complete loss of FATP1 expression was observed in cells expressing FATP1 sequence-specific shRNA (FATP1 kd), indicating that the protein is not required for adipose conversion. Expression of shRNA directed toward FATP4 (FATP4 kd) produced a cell line exhibiting ∼10% of the control FATP4 level (**Fig. 1**). Immunoblotting of protein extracts from FATP1 kd, FATP4 kd, and control cells revealed an ∼50% increase in the expression of PPARγ and an ∼20% increase in C/EBPα protein. Despite the increase in expression of key adipogenic transcription factors, the expression of proteins regulated by PPARγ and implicated in some facet of fatty acid influx (CD36, ACSL1, FATP4/FATP1) and/or the PPARγ target genes adipocyte fatty acid binding protein (AFABP/aP2), CD36, and FATP were unchanged in abundance in both cell lines (Fig. 1).

Both FATP1 kd and FATP4 kd adipocytes exhibited reduced accumulation of triacylglycerol. Oil Red O staining
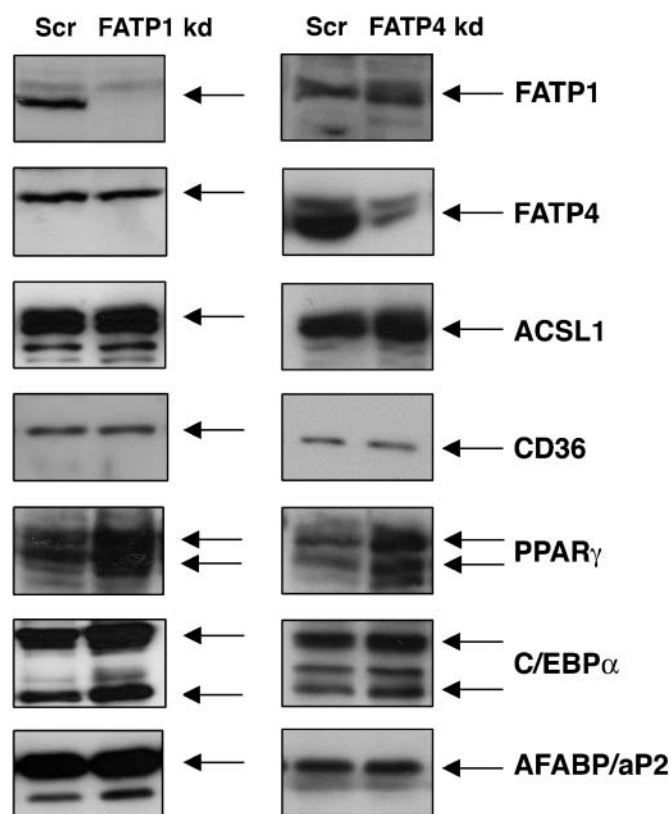

Fig. 1. Immunoblot analysis of cell extracts from day 9 3T3-L1 adipocytes expressing fatty acid transport protein 1 (FATP1) short hairpin RNA (shRNA) [FATP1 kd (for knockdown)], FATP4 shRNA (FATP4 kd), or scrambled sequence shRNA (Scr) as a control. The blot is representative of three separate experiments. ACSL1, acyl-coenzyme A synthetase 1; AFABP/aP2, adipocyte fatty acid binding protein; CD36, fatty acid translocase; C/EBPα, CCAAT/enhancer binding protein α; PPARγ, peroxisome proliferator-activated receptor γ.

of triacylglycerol droplets was reduced markedly, exhibiting smaller lipid droplet sizes in FATP1 kd and FATP4 kd 3T3-L1 adipocytes relative to the scrambled control (which was not different from uninfected or vector-infected adipocytes; results not shown). Consistent with the reduced Oil Red O staining, FATP1 kd and FATP4 kd cells exhibited decreased triacylglycerol, diacylglycerol, and monoacylglycerol levels. FATP4 kd cells, but not FATP1 kd cells, exhibited a decrease in free fatty acid level (**Fig. 2**).

FATP1 is an ACSL with broad substrate specificity (C16:0 vs. C24:0 esterification) but a rather low enzymatic reaction rate relative to other fatty acid CoA ligases. Conversely, FATP4 has a high ACSL reaction rate relative to FATP1 and ACSL1 and has a substrate preference for very long-chain (C24:0) over long-chain (C16:0) fatty acids (21). To evaluate the effect of FATP1 kd and FATP4 kd on total cellular ACSL activity, extracts were prepared and assayed for fatty acid esterification using a variety of fatty acid substrates. As shown in **Table 1**, kd of FATP1 resulted in an ∼10–15% decrease in cellular C16:0, C18:1, and C20:4 esterification activity but essentially no change in total cellular C24:0 ACSL activity. Compared with FATP1 kd adipocytes, FATP4 kd adipocytes displayed a 20–25% decrease in cellular C16:0, C18:1, and C20:4 ACSL activities and no change in total cellular C24:0 ACSL. The decrease in total ACSL activity for either kd cell line (10–25%) correlated well with the measured decrease in triacylglycerol, diacylglycerol, and monoacylglycerol levels in the cell (Fig. 2).

Because there was a significant, albeit modest, decrease in total cellular ACSL activities as well as triacylglycerol levels, we assessed the role that FATP1 and FATP4 may play in fatty acid uptake. Stahl and colleagues (5) have reported that insulin stimulates the translocation of FATP1 from intracellular sites to the plasma membrane. To assess this, 3T3-L1 adipocytes were serum-starved and then incubated with or without insulin for 30 min, and the expression of FATP1, FATP4, and GLUT4 was evaluated using secondary immunofluorescence. As shown in **Fig. 3**, the majority of immunoreactive GLUT4 translocated to the plasma membrane, as did some immunoreactive FATP1 (estimated to be 10%). In contrast to FATP1 and GLUT4, FATP4 did not appear to be localized to the plasma membrane under basal conditions and did not translocate to the plasma membrane in the presence of insulin.

To parallel the translocation studies for FATP1 and FATP4 shown immunochemically with biochemical analysis, the cellular influx of [3H]-labeled fatty acids of different chain lengths was evaluated under basal and insulin-stimulated conditions. As shown in **Fig. 4A**, under basal conditions, compared with control cells, FATP1 kd adipocytes displayed an ∼25% decrease in fatty acid uptake for [3H]palmitic acid, [3H]oleic acid, and [3H]arachidonic acid. Because of its poor solubility, influx studies with C24:0 were not performed. For control 3T3-L1 adipocytes, insulin stimulation led to an ∼15–40% increase in fatty acid influx for [3H]palmitic acid, [3H]oleic acid, and [3H]arachidonic acid. The increase in [3H]palmitic and [3H]oleic acid uptake in response to insulin was com-
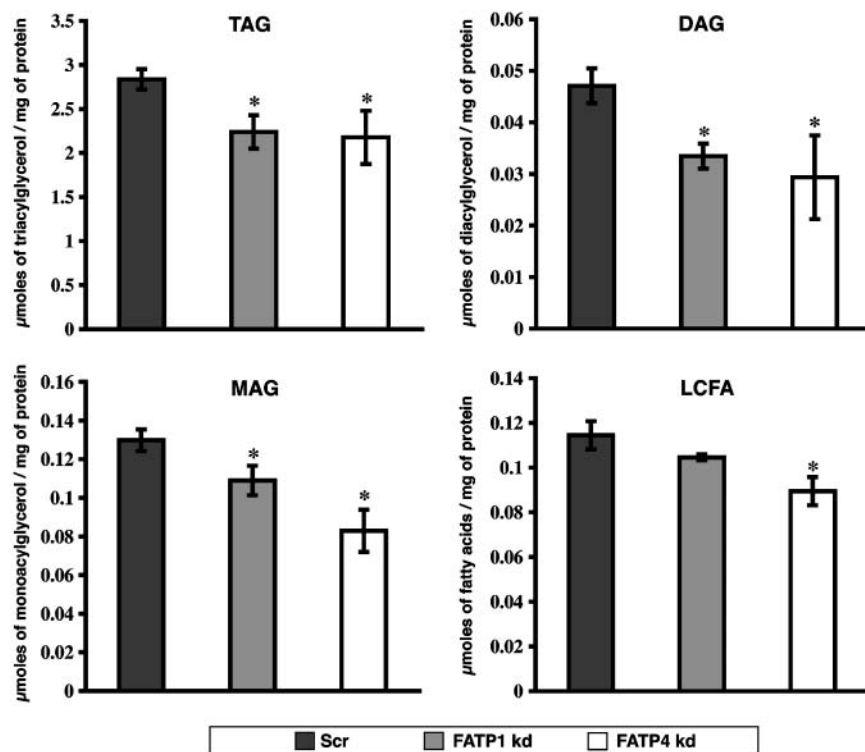
Fig. 2. Quantitative determination of triacylglycerol (TAG), diacylglycerol (DAG), monoacylglycerol (MAG), and long-chain fatty acid (LCFA) content in FATP1 kd, FATP4 kd, and control 3T3-L1 adipocytes. The data shown are representative of three separate experiments. * $P < 0.05$ relative to scrambled control cultures (Scr). Error bars indicate SD.

pletely lost in FATP1 kd cells, indicating a crucial role of FATP1 in insulin-stimulated fatty acid influx. This is consistent with the translocation of FATP1 to the plasma membrane in response to insulin (Fig. 3) and is indicative of the role of FATP1 in fatty acid uptake as a critical function of its cellular location. The increase in [³H]arachidonic acid uptake with insulin stimulation in FATP1 kd cells is not completely lost but is decreased by ∼20% compared with the response of control cells to insulin. This suggests that in addition to FATP1, another ACSL with substrate specificity for arachidonic acid may facilitate its cellular uptake.

TABLE 1. Analysis of ACSL activities of cellular extracts from 3T3-L1 adipocytes expressing FATP1 shRNA and FATP4 shRNA compared with the scrambled control

Substrate	Scrambled Control	FATP1 kd	FATP4 kd
	nmol/min/mg protein		
C16:0	168.0 ± 2.5	140.3 ± 6.1[a]	134.1 ± 6.4[a]
C18:1	191.8 ± 5.2	155.8 ± 4.9[a]	149.6 ± 3.1[a]
C20:4	131.2 ± 2.7	118.6 ± 3.1[a]	106.3 ± 3.7[a]
C24:0	7.7 ± 1.2	8.7 ± 1.5	7.2 ± 1.7

ACSL, acyl-coenzyme A synthetase; FATP1, fatty acid transport protein 1; kd, knockdown. ACSL activities of cell extracts from day 8 differentiated 3T3-L1 adipocytes were assayed for esterification of palmitic acid (C16:0), oleic acid (C18:1), arachidonic acid (C20:4), and lignoceric acid (C24:0) and are expressed as nmol/min/mg total protein. Data are representative of three independent experiments.
[a] $P < 0.05$ comparing experimental with scrambled control values.

Despite FATP4 having the highest ACSL enzyme reaction rates relative to other cellular ACSLs, such as FATP1 and ACSL1, FATP4 kd adipocytes did not demonstrate any change in [³H]palmitic, [³H]oleic, or [³H]arachidonic acid uptake relative to the control cells under both basal and insulin-stimulated conditions (Fig. 4B). This is in agreement with the results of fatty acid influx studies carried out with different stable HEK-293 cell lines expressing varying amounts of FATP4 (**Fig. 5**). The amount of FATP4 expressed by each individual cell line was analyzed by immunoblotting and densitometric analysis and represented as arbitrary FATP4 units. As shown in Fig. 5A, the ACSL activity for a C24:0 fatty acid substrate analyzed with cell extracts from different HEK-293 cell lines varied proportionately to the amount of FATP4 being expressed. However, the varying expression levels of FATP4 in HEK-293 cells did not affect the rate of cellular fatty acid influx for [³H]oleic acid (Fig. 5B). Thus, unlike FATP1, FATP4 is not translocated to the plasma membrane in response to insulin and is not rate-limiting for basal or insulin-stimulated fatty acid uptake.

To contrast the results of fatty acid influx observed in FATP1 kd and FATP4 kd adipocytes with measures of fatty acid efflux, control, FATP1 kd, and FATP4 kd adipocytes were evaluated for their ability to carry out basal and forskolin-stimulated lipolysis. Lipolysis was measured as the amount of glycerol and fatty acids released from cells as a result of triglyceride hydrolysis. As shown in **Fig. 6**,
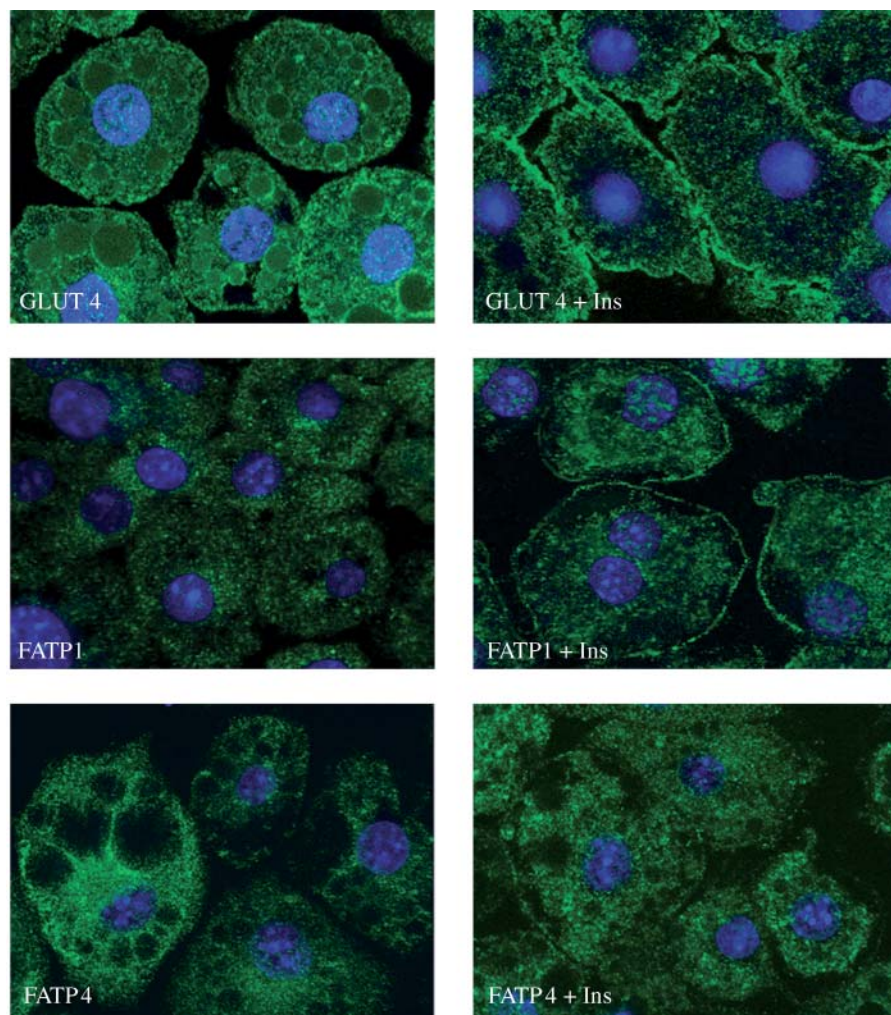
Fig. 3. Immunolocalization by confocal microscopy of FATP1 and FATP4 compared with the glucose transporter GLUT4 under basal and insulin-stimulatory conditions in 3T3-L1 adipocytes. Serum-starved day 6 3T3-L1 adipocytes were treated with or without 50 ng/ml insulin for 30 min. Fluorescent detection was enabled by incubation with the secondary antibody Alexa Fluor 488 donkey anti-rabbit IgG (green) and subsequent nuclei staining with TOPRO3 (blue).

glycerol and fatty acid release in control, FATP1 kd, and FATP4 kd adipocytes exhibited no significant differences between all cell types under forskolin-stimulated conditions. Consistent with the smaller droplet size, FATP1 kd adipocytes exhibited reduced basal fatty acid release. In contrast, FATP4 kd adipocytes exhibited an ~30% increase in glycerol and an ~75% increase in fatty acid release during basal lipolysis.

Insulin stimulated the translocation of FATP1 to the plasma membrane, which correlated with the increase in fatty acid uptake observed in control adipocytes that was diminished in FATP1 kd adipocytes. As opposed to FATP1, FATP4 remained localized to intracellular membranes even with insulin stimulation and did not affect fatty acid uptake. To further understand the unique roles of these two fatty acid transporters in fat, we analyzed the differences in the metabolism of palmitate into various complex lipid pools after cellular influx in FATP1 kd, FATP4 kd, and control adipocytes under basal and insulin-stimulatory conditions. As shown in **Table 2**, under both basal and insulin-stimulated conditions, the vast majority of the fatty acid (>90%) is activated to CoA esters and incorporated into neutral lipids, primarily triacylglycerol. A very small fraction (only 2%) of fatty acids are retained intracellularly without being metabolized (Table 2). Comparison of lipid profiles between FATP1 kd and control adipocytes indicated that although there was an ~15% decrease in total fatty acid uptake in the FATP1 kd adipocytes under basal conditions, there was essentially a 100% decrease in the insulin-stimulated fraction of uptake. A corresponding decrease in fatty acyl-CoA levels and triacylglycerol synthesis was observed in FATP1 kd adipocytes compared with the control. These results are consistent with a requirement for FATP1 in the insulin-stimulated component of LCFA influx and triacylglycerol synthesis in 3T3-L1 adipocytes. Although FATP4 did not play a role in fatty acid uptake under basal conditions, an ~40% decrease in the fatty acyl-CoA pools

Fig. 5. Comparative analysis of cellular lignoceryl (C24:0) CoA synthetase activity (A) and oleic acid (C18:1) influx (B) carried out with different stable HEK-293 cell lines expressing varying amounts of FATP4. The amounts of FATP4 expressed by each individual cell line were analyzed by immunoblotting and densitometry and are represented as arbitrary FATP4 units. Error bars indicate SD.

however, no change was observed in fatty acyl-CoA levels or in any other complex lipid class pool analyzed.

Because both FATP1 kd and FATP4 kd adipocytes had reduced lipid contents compared with the control cells, and reduced triacylglycerol deposition is often correlated with increased hexose uptake (31, 32), we evaluated the loss of each FATP isoform on basal and insulin-stimulated 2-deoxyglucose uptake. Interestingly, there was an ∼30% increase in basal and insulin-stimulated glucose uptake in FATP1 kd adipocytes compared with the control (**Fig. 7**). The increase in glucose uptake (∼6-fold) upon insulin stimulation was the same in both adipocyte cell types. Similarly, when control and FATP4 kd cells were evaluated for 2-deoxyglucose uptake, cells lacking FATP4 exhibited an ∼20% increase in insulin-stimulated uptake but no change in basal glucose uptake.

DISCUSSION

Since its discovery in 1994, FATP1 has been investigated for its role in fatty acid transport and regulation. Various overexpression systems and a knockout mouse model have implicated FATP1 in fatty acid uptake (13, 15). FATP1 transcription is regulated by multiple systems: negatively by insulin and positively by a PPARγ-dependent mechanism (33, 34). Consistent with this, FATP1 expression in muscle and fat is increased in obese diabetic animals, and mice
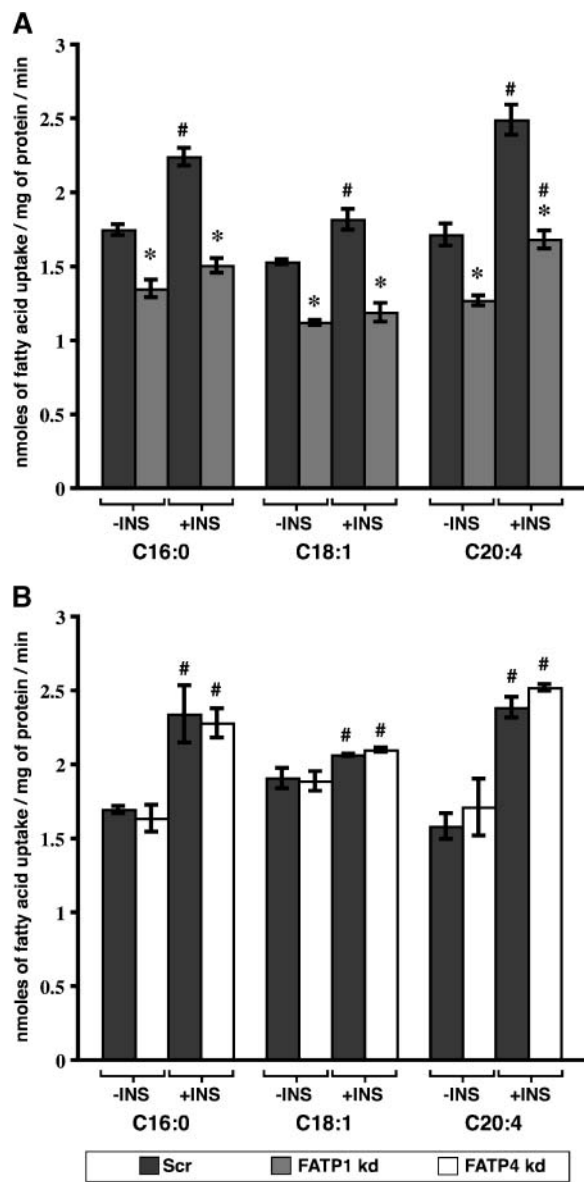
Fig. 4. Cellular uptake of different chain-length ^{3}H-labeled fatty acids in FATP1 kd (A) and FATP4 kd (B) 3T3-L1 adipocytes compared with the scrambled control (Scr). Day 9 differentiated serum starved 3T3-L1 adipocytes in the absence (−INS) and presence (+INS) of 50 nM insulin were incubated with 50 μM [^{3}H]palmitic acid (C16:0), oleic acid (C18:1), or arachidonic acid (C20:4) bound to albumin to produce a free unbound concentration of LCFA of 5 nM. Influx reactions were terminated, and the incorporated radioactivity was determined as described in Materials and Methods. A: FATP1 kd (gray bars) compared with scrambled (control) adipocytes (black bars). B: FATP4 kd adipocytes (white bars) compared with scrambled (control) adipocytes (black bars). The data shown are representative of three separate experiments. * $P < 0.05$ relative to scrambled control cultures; # $P < 0.05$ relative to non-stimulatory basal conditions. Error bars indicate SD.

was observed in FATP4 kd adipocytes relative to the control (**Table 3**). The mechanistic basis for this is unclear, but it may suggest that other proteins may be rate-limiting for LCFA influx but that FATP4 plays a role in internalized lipid esterification. With insulin stimulation,
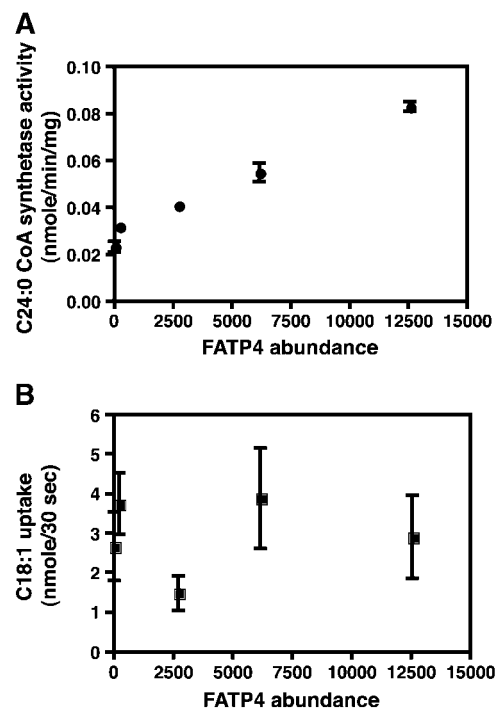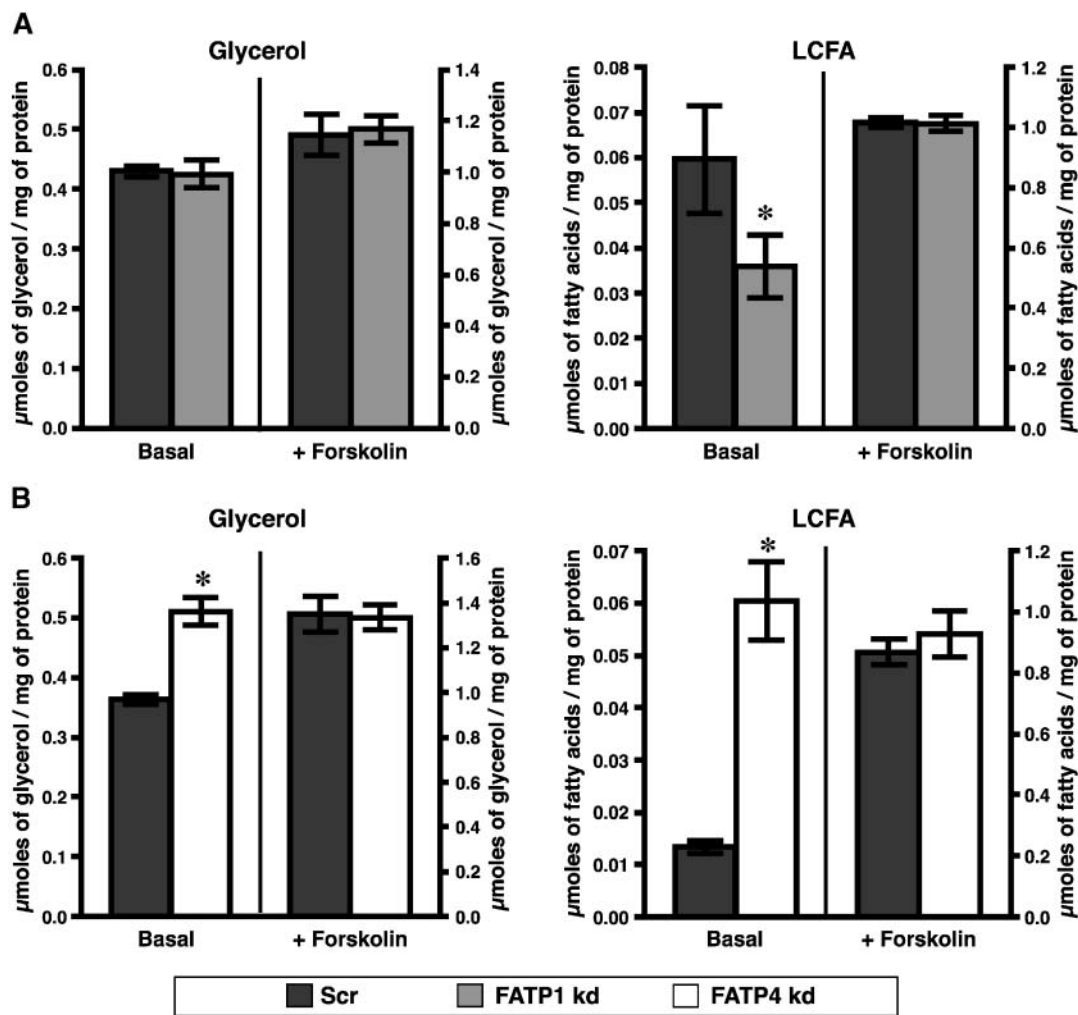
Fig. 6. Analysis of basal and forskolin-stimulated lipolysis in FATP1 kd (A) and FATP4 kd (B) 3T3-L1 adipocytes compared with the scrambled control (Scr). Day 8 differentiated 3T3-L1 adipocytes were treated for 2 h in the absence or presence of 20 μM forskolin, and aliquots of medium were withdrawn for measurement of glycerol and fatty acid release. The data shown are representative of three separate experiments. * $P < 0.05$ relative to scrambled control cultures. Error bars indicate SD.

null for FATP1 exhibit reduced skeletal muscle LCFA uptake and resistance to high-fat diet-induced insulin resistance (15, 35). In fat cells, rosiglitazone, a PPARγ agonist, increases the expression of both CD36 and FATP1, suggesting that the lipid-lowering effects of this insulin-sensitizing drug may be exerted at the level of adipose LCFA influx (36). Thus, the identification of a precise role for FATP1 in fatty acid influx may be crucial to understanding the mechanism of the beneficial insulin-sensitizing effects of this widely used class of drugs.

Although loss- and gain-of-function model systems have defined a role of FATP4 as a major intestinal fatty acid transporter and in the maintenance of the skin's epidermal barrier function, its role in adipocyte fatty acid uptake and lipid metabolism is less well defined. FATP4 expression in primary human placental trophoblasts is regulated by PPARγ and retinoid X receptor (37). Genetic polymorphisms in humans support a role of FATP4 in insulin sensitivity (23). Indeed, heterozygotes for a G209S polymorphism (serine frequency of 5%) exhibited lower body mass index, lower serum fatty acids and triglycerides, reduced systolic blood pressure, and diminished insulin levels. FATP4 expression levels correlate with acquired obesity that is independent of genetic background (24).

Using a lentivirus-delivered RNAi kd technique, we succeeded in suppressing the FATP1/FATP4 protein expression levels in 3T3-L1 adipocytes essentially quantitatively. Interestingly, loss of FATP1 and FATP4 independently led to an increase in the expression of both C/EBPα and PPARγ. The mechanistic basis for this increase is not clear but may be related to reduced PPARγ degradation affecting negative feedback regulation of the receptor, as opposed to changes in activating factors (38). Despite the increased expression of these key transcription factors, other PPARγ targets were not increased in expression, including AFABP/aP2, ACSL1, and CD36. Knockout of FATP1 or FATP4 in 3T3-L1 adipocytes led to small changes in total cellular long-chain ACSL activities without causing any change in cellular very long-chain ACSL activity.

TABLE 2. Complex lipid synthesis in FATP1 kd and scrambled 3T3-L1 adipocytes

	Basal		Insulin	
	Scrambled Control	FATP1 kd	Scrambled Control	FATP1 kd
Variable	nmol/mg	nmol/mg	nmol/mg	nmol/mg
Total incorporation	6.78 ± 0.25	5.83 ± 0.21[a]	9.00 ± 0.38	6.22 ± 0.26[a]
Cellular lipid class				
Fatty acids	0.09 ± 0.01	0.07 ± 0.003[a]	0.07 ± 0.01	0.04 ± 0.01[a]
Fatty acyl-CoA	0.71 ± 0.03	0.55 ± 0.03[a]	0.98 ± 0.07	0.78 ± 0.07[a]
Neutral lipids	4.32 ± 0.12	3.62 ± 0.10[a]	6.53 ± 0.24	4.38 ± 0.45[a]
Neutral lipid class				
Triacylglycerol	2.51 ± 0.13	2.13 ± 0.09[a]	4.69 ± 0.03	3.07 ± 0.24[a]
Diacylgylcerol	0.13 ± 0.02	0.14 ± 0.01	0.53 ± 0.07	0.46 ± 0.02[a]
Monoacylglycerol	0.26 ± 0.02	0.28 ± 0.01	0.83 ± 0.09	0.71 ± 0.01[a]

Serum-starved 3T3-L1 adipocytes were incubated with [^{3}H]palmitic acid bound to albumin for 5 min at 37°C in the absence (basal) and presence of 100 nM insulin. Cellular lipids were extracted and fractionated, and the incorporation of radiolabel into various lipid pools was determined. The results are representative of three independent experiments.

[a] $P < 0.05$ comparing experimental with scrambled control values.

Depletion of FATP1 expression resulted in an essentially quantitative loss in insulin-stimulated oleic and palmitic acid uptake and an ~20% decrease in insulin-stimulated arachidonic acid influx. Significant reduction in FATP1 expression level, however, caused only a small ~25% decrease in basal LCFA influx for all fatty acids analyzed. Depletion of FATP4, on the other hand, did not affect either basal or insulin-stimulated fatty acid uptake, and overexpression of FATP4 in HEK-293 cells did not affect cellular fatty acid influx rates. We (Fig. 3) and others (5) have shown that in 3T3-L1 adipocytes, insulin can stimulate the translocation of FATP1 from intracellular membranes to the plasma membrane. However, as opposed to GLUT4, only a small fraction (estimated to be <10%) of total FATP1 translocated. As such, the increase in the relative abundance of the enzyme at the plasma membrane correlates with increased LCFA influx and may be crucial to regulation of the fatty acid transport function of FATP1. Our results with FATP4 kd adipocytes indicate that although FATP4 has a high ACSL reaction rate relative to FATP1 and ACSL1, it is localized to internal membranes and not the plasma membrane, which could be the reason why it does not contribute to either insulin-stimulated or basal fatty acid uptake. In contrast to our studies, FATP4

overexpressed in COS cells (which too was localized to the endoplasmic reticulum) did result in a net increase in LCFA influx (39). It is not clear whether these contradictory findings are the result of differences in the absolute level of FATP4 expression, differences in experimental assay conditions, or simply a difference in the cell culture system used.

Our results do not eliminate the possibility of other proteins functioning in insulin-stimulated LCFA influx. Indeed, insulin-stimulated arachidonic acid uptake is not completely lost in FATP1 kd adipocytes, suggesting that another ACSL could participate in insulin-stimulated arachidonic acid fatty acid influx. ACSL1, which has been suggested to form a complex with FATP1 (6), could participate in some facet of insulin-stimulated or basal LCFA influx. What is not clear in this study is what facilitates basal LCFA influx in adipocytes. Insulin stimulation of LCFA influx is fatty acid-specific and is quantitatively modest (~15–40%) relative to insulin-stimulated hexose uptake (5- to 20-fold). Other factors (caveolin-1, CD36, ACSL1) are likely contributors to basal LCFA influx.

Fatty acid reesterification within the adipocyte can vary by 30–70% during periods of basal lipolysis, affecting the net output of lipid from the adipocyte (40). The basal

TABLE 3. Complex lipid synthesis in FATP4 kd and scrambled 3T3-L1 adipocytes

	Basal		Insulin	
	Scrambled Control	FATP4 kd	Scrambled Control	FATP4 kd
Variable	nmol/mg	nmol/mg	nmol/mg	nmol/mg
Cellular lipid class				
Fatty acids	0.043 ± 0.01	0.047 ± 0.002	0.042 ± 0.01	0.032 ± 0.01
Fatty acyl-CoA	0.93 ± 0.04	0.59 ± 0.04[a]	1.01 ± 0.05	0.94 ± 0.06
Neutral lipids	3.06 ± 0.09	2.83 ± 0.25	4.13 ± 0.30	4.10 ± 0.21
Neutral lipid class				
Triacylglycerol	1.21 ± 0.05	1.31 ± 0.05	1.92 ± 0.08	1.68 ± 0.18
Diacylglycerol	0.09 ± 0.01	0.09 ± 0.01	0.07 ± 0.01	0.10 ± 0.03
Monoacylglycerol	0.21 ± 0.04	0.16 ± 0.03	0.62 ± 0.01	0.60 ± 0.02

Serum-starved 3T3-L1 adipocytes were incubated with [^{3}H]palmitic acid bound to albumin in the absence (basal) and presence of 100 nM insulin. Cellular lipids were extracted and fractionated, and the incorporation of radiolabel into various lipid pools was determined. The results are representative of three independent experiments.

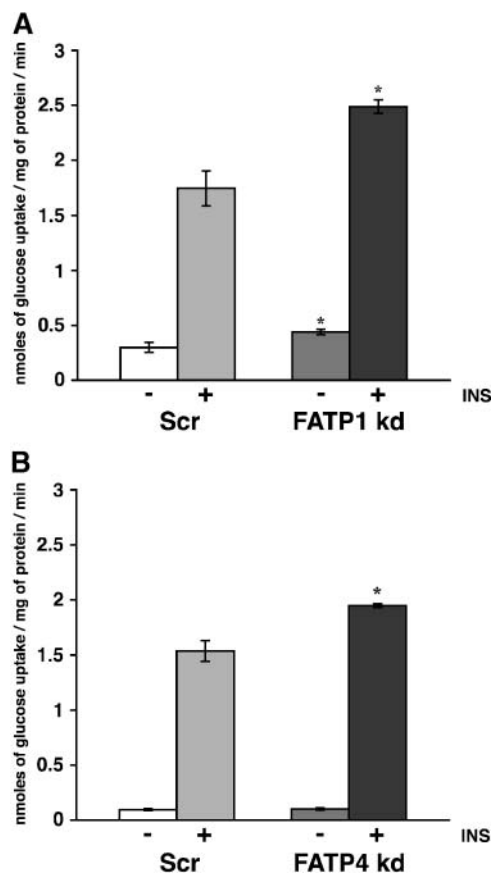[a] $P < 0.05$ comparing experimental with scrambled control values.

Fig. 7. Basal and insulin-stimulated 2-deoxyglucose uptake in FATP1 kd (A) and FATP4 kd (B) 3T3-L1 adipocytes compared with the scrambled control (Scr). Day 9 differentiated serum-starved 3T3-L1 adipocytes were incubated with [^{14}C]2-deoxy-D-glucose in the absence and presence of 100 nM insulin as described in Materials and Methods, and glucose influx was determined. * P < 0.05 relative to scrambled control cultures. Error bars indicate standard deviation.

lipolytic rate is proportional to triacylglycerol deposition, and in general, larger fat cells have greater rates of basal lipolysis than do small fat cells (41). However, the mechanism and the components involved in basal lipolysis are less well characterized. Here, we show that under basal lipolytic conditions, FATP4 kd adipocytes exhibited an increase in the amount of glycerol and fatty acid released relative to a control scrambled cell line. One explanation for this is that the ACSL activity of FATP4 may facilitate some component of the CoA-dependent reesterification of fatty acids derived from basal lipolysis of the triacylglycerol droplet. Other ACSLs, such as ACSL1, which has been found to be associated with the lipid droplet, may also play a role in fatty acid reesterification during basal lipolysis (42). However, alternative explanations also exist.

Experiments analyzing the distribution of [^{3}H]palmitate into various complex lipids indicate that in 3T3-L1 adipocytes, the vast majority of incoming fatty acids are converted to their acyl-CoA derivatives and preferentially shunted into the triacylglycerol synthesis pathway. In FATP1 kd adipocytes, a decrease in LCFA influx was coupled with reduced acyl-CoA levels as well as triacylglycerol, diacylglycerol, and monoacylglycerol pools. Importantly, the LCFA pool was not increased but also similarly reduced, consistent with the model that the ACSL activity of FATP1 is critical for facilitating LCFA influx. These results are in agreement with the observations of Stuhlsatz-Krouper, Bennett, and Schaffer (43), who have shown that mutation of FATP1 serine 250 to alanine not only reduced the catalytic activity of the enzyme but also eliminated LCFA influx, implying that catalysis is functionally linked to uptake. In contrast to FATP1 kd adipocytes, FATP4 kd adipocytes revealed no change in basal or insulin-stimulated cellular fatty acid influx. Under basal conditions, FATP4 kd adipocytes revealed a decrease in the incorporation of [^{3}H]palmitate into acyl-CoA pools but not triglyceride pools. The mechanistic basis for this is undetermined but suggests that under basal conditions, FATP4 functions in LCFA esterification but that other proteins may mediate the rate-controlling steps in internalization. With insulin stimulation, however, no changes in the fatty acyl-CoA pools incorporating [^{3}H]palmitate were observed, consistent with the anti-lipolytic effects of the hormone insulin and the proposed role of FATP4 in basal lipolysis. Stralfors and colleagues (44) recently reported that the conversion of fatty acids to triacylgylcerol occurs on or around the plasma membrane of rat adipocytes. Our results reported here are consistent with this view and imply that acyl-CoA production at the plasma membrane may be mechanistically linked to triacylglycerol synthesis via some type of organized lipid synthesis machinery.

Both FATP1 kd and FATP4 kd adipocytes exhibited increased insulin-stimulated glucose uptake. FATP1 knockout mice exhibit a similar increase in insulin-stimulated glucose uptake in soleus muscle compared with wild-type mice (45). Although the increase in glucose uptake may be quantitatively modest, over time small changes in glucose uptake have important metabolic consequences, including insulin sensitivity, such as that observed in FATP1 knockout mice and humans expressing either the S209 or G209 polymorphism of the *FATP4* gene. In both FATP1 kd and FATP4 kd cells, the abundance of several potential lipid regulators (diacylglycerol, LCFA) (46) of insulin signaling is altered. Consequently, the development of FATP1/FATP4 kd adipocytes may provide an opportunity to identify lipid-derived signaling pathways that originate from altered triacylglycerol levels that affect insulin resistance in adipocytes.

In summary, although FATP1 and FATP4 both possess ACSL enzyme activities and share 60.3% sequence identity, each has unique functional roles in the adipocyte. FATP1 plays a minor role in basal fatty acid uptake, and by virtue of its translocation to the plasma membrane from intracellular membranes in response to insulin, plays a major role in insulin-stimulated fatty acid uptake. FATP4 is an intracellular ACSL that does not play a rate-limiting role in either basal or insulin-stimulated fatty acid uptake and may be involved in fatty acid reesterification after lipolysis. FATP1 and FATP4, by virtue of their distinctive

cellular locations and roles, affect triglyceride lipid droplet size and other complex lipid pools, both of which have been implicated in the development of obesity and insulin resistance.▉

REFERENCES

1. Frayn, K. N. 2005. Obesity and metabolic disease: is adipose tissue the culprit? *Proc. Nutr. Soc.* **64:** 7–13.

2. Lazar, M. A. 2005. How obesity causes diabetes: not a tall tale. *Science.* **307:** 373–375.

3. Zhang, J., M. Fu, T. Cui, C. Xiong, K. Xu, W. Zhong, Y. Xiao, D. Floyd, J. Liang, E. Li, et al. 2004. Selective disruption of PPARgamma 2 impairs the development of adipose tissue and insulin sensitivity. *Proc. Natl. Acad. Sci. USA.* **101:** 10703–10708.

4. Coburn, C. T., F. F. Knapp, Jr., M. Febbraio, A. L. Beets, R. L. Silverstein, and N. A. Abumrad. 2000. Defective uptake and utilization of long chain fatty acids in muscle and adipose tissues of CD36 knockout mice. *J. Biol. Chem.* **275:** 32523–32529.

5. Stahl, A., J. G. Evans, S. Pattel, D. Hirsch, and H. F. Lodish. 2002. Insulin causes fatty acid transport protein translocation and enhanced fatty acid uptake in adipocytes. *Dev. Cell.* **2:** 477–488.

6. Richards, M. R., J. D. Harp, D. S. Ory, and J. E. Schaffer. 2006. Fatty acid transport protein 1 and long-chain acyl coenzyme A synthetase 1 interact in adipocytes. *J. Lipid Res.* **47:** 665–672.

7. Zhou, S. L., D. Stump, C. L. Kiang, L. M. Isola, and P. D. Berk. 1995. Mitochondrial aspartate aminotransferase expressed on the surface of 3T3-L1 adipocytes mediates saturable fatty acid uptake. *Proc. Soc. Exp. Biol. Med.* **208:** 263–270.

8. Trigatti, B. L., R. G. Anderson, and G. E. Gerber. 1999. Identification of caveolin-1 as a fatty acid binding protein. *Biochem. Biophys. Res. Commun.* **255:** 34–39.

9. Hall, A. M., A. J. Smith, and D. A. Bernlohr. 2003. Characterization of the acyl-CoA synthetase activity of purified murine fatty acid transport protein 1. *J. Biol. Chem.* **278:** 43008–43013.

10. Stahl, A. 2004. A current review of fatty acid transport proteins (SLC27). *Pflugers Arch.* **447:** 722–727.

11. Schaffer, J. E., and H. F. Lodish. 1994. Expression cloning and characterization of a novel adipocyte long chain fatty acid transport protein. *Cell.* **79:** 427–436.

12. Hatch, G. M., A. J. Smith, F. Y. Xu, A. M. Hall, and D. A. Bernlohr. 2002. FATP1 channels exogenous FA into 1,2,3-triacyl-sn-glycerol and down-regulates sphingomyelin and cholesterol metabolism in growing 293 cells. *J. Lipid Res.* **43:** 1380–1389.

13. Chiu, H. C., A. Kovacs, R. M. Blanton, X. Han, M. Courtois, C. J. Weinheimer, K. A. Yamada, S. Brunet, H. Xu, J. M. Nerbonne, et al. 2005. Transgenic expression of fatty acid transport protein 1 in the heart causes lipotoxic cardiomyopathy. *Circ. Res.* **96:** 225–233.

14. Faergeman, N. J., C. C. DiRusso, A. Elberger, J. Knudsen, and P. N. Black. 1997. Disruption of the *Saccharomyces cerevisiae* homologue to the murine fatty acid transport protein impairs uptake and growth on long-chain fatty acids. *J. Biol. Chem.* **272:** 8531–8538.

15. Kim, J. K., R. E. Gimeno, T. Higashimori, H. J. Kim, H. Choi, S. Punreddy, R. L. Mozell, G. Tan, A. Stricker-Krongrad, D. J. Hirsch, et al. 2004. Inactivation of fatty acid transport protein 1 prevents fat-induced insulin resistance in skeletal muscle. *J. Clin. Invest.* **113:** 756–763.

16. Herrmann, T., F. Buchkremer, I. Gosch, A. M. Hall, D. A. Bernlohr, and W. Stremmel. 2001. Mouse fatty acid transport protein 4 (FATP4): characterization of the gene and functional assessment as a very long chain acyl-CoA synthetase. *Gene.* **270:** 31–40.

17. Stahl, A., D. J. Hirsch, R. E. Gimeno, S. Punreddy, P. Ge, N. Watson, S. Patel, M. Kotler, A. Raimondi, L. A. Tartaglia, et al. 1999. Identification of the major intestinal fatty acid transport protein. *Mol. Cell.* **4:** 299–308.

18. Gimeno, R. E., D. J. Hirsch, S. Punreddy, Y. Sun, A. M. Ortegon, H. Wu, T. Daniels, A. Stricker-Krongrad, H. F. Lodish, and A. Stahl. 2003. Targeted deletion of fatty acid transport protein-4 results in early embryonic lethality. *J. Biol. Chem.* **278:** 49512–49516.

19. Herrmann, T., F. van der Hoeven, H. J. Grone, A. F. Stewart, L. Langbein, I. Kaiser, G. Liebisch, I. Gosch, F. Buchkremer, W. Drobnik, et al. 2003. Mice with targeted disruption of the fatty acid transport protein 4 (Fatp 4, Slc27a4) gene show features of lethal restrictive dermopathy. *J. Cell Biol.* **161:** 1105–1115.

20. Moulson, C. L., D. R. Martin, J. J. Lugus, J. E. Schaffer, A. C. Lind, and J. H. Miner. 2003. Cloning of wrinkle-free, a previously uncharacterized mouse mutation, reveals crucial roles for fatty acid transport protein 4 in skin and hair development. *Proc. Natl. Acad. Sci. USA.* **100:** 5274–5279.

21. Hall, A. M., B. M. Wiczer, T. Herrmann, W. Stremmel, and D. A. Bernlohr. 2005. Enzymatic properties of purified murine fatty acid transport protein 4 and analysis of acyl-CoA synthetase activities in tissues from FATP4 null mice. *J. Biol. Chem.* **280:** 11948–11954.

22. Herrmann, T., H. J. Grone, L. Langbein, I. Kaiser, I. Gosch, U. Bennemann, D. Metzger, P. Chambon, A. F. Stewart, and W. Stremmel. 2005. Disturbed epidermal structure in mice with temporally controlled fatp4 deficiency. *J. Invest. Dermatol.* **125:** 1228–1235.

23. Gertow, K., M. Bellanda, P. Eriksson, S. Boquist, A. Hamsten, M. Sunnerhagen, and R. M. Fisher. 2004. Genetic and structural evaluation of fatty acid transport protein-4 in relation to markers of the insulin resistance syndrome. *J. Clin. Endocrinol. Metab.* **89:** 392–399.

24. Gertow, K., K. H. Pietilainen, H. Yki-Jarvinen, J. Kaprio, A. Rissanen, P. Eriksson, A. Hamsten, and R. M. Fisher. 2004. Expression of fatty-acid-handling proteins in human adipose tissue in relation to obesity and insulin resistance. *Diabetologia.* **47:** 1118–1125.

25. Student, A. K., R. Y. Hsu, and M. D. Lane. 1980. Induction of fatty acid synthetase synthesis in differentiating 3T3-L1 preadipocytes. *J. Biol. Chem.* **255:** 4745–4750.

26. Stewart, S. A., D. M. Dykxhoorn, D. Palliser, H. Mizuno, E. Y. Yu, D. S. An, D. M. Sabatini, I. S. Chen, W. C. Hahn, P. A. Sharp, et al. 2003. Lentivirus-delivered stable gene silencing by RNAi in primary cells. *RNA.* **9:** 493–501.

27. Richieri, G. V., A. Anel, and A. M. Kleinfeld. 1993. Interactions of long-chain fatty acids and albumin: determination of free fatty acid levels using the fluorescent probe ADIFAB. *Biochemistry.* **32:** 7574–7580.

28. Kaluzny, M. A., L. A. Duncan, M. V. Merritt, and D. E. Epps. 1985. Rapid separation of lipid classes in high yield and purity using bonded phase columns. *J. Lipid Res.* **26:** 135–140.

29. Nagamatsu, K., S. Soeda, M. Mori, and Y. Kishimoto. 1985. Lignoceroyl-coenzyme A synthetase from developing rat brain: partial purification, characterization and comparison with palmitoyl-coenzyme A synthetase activity and liver enzyme. *Biochim. Biophys. Acta.* **836:** 80–88.

30. Jiang, Z. Y., Q. L. Zhou, K. A. Coleman, M. Chouinard, Q. Boese, and M. P. Czech. 2003. Insulin signaling through Akt/protein kinase B analyzed by small interfering RNA-mediated gene silencing. *Proc. Natl. Acad. Sci. USA.* **100:** 7569–7574.

31. Yamauchi, T., J. Kamon, H. Waki, Y. Terauchi, N. Kubota, K. Hara, Y. Mori, T. Ide, K. Murakami, N. Tsuboyama-Kasaoka, et al. 2001. The fat-derived hormone adiponectin reverses insulin resistance associated with both lipoatrophy and obesity. *Nat. Med.* **7:** 941–946.

32. de Souza, C. J., M. Eckhardt, K. Gagen, M. Dong, W. Chen, D. Laurent, and B. F. Burkey. 2001. Effects of pioglitazone on adipose tissue remodeling within the setting of obesity and insulin resistance. *Diabetes.* **50:** 1863–1871.

33. Hui, T. Y., B. I. Frohnert, A. J. Smith, J. E. Schaffer, and D. A. Bernlohr. 1998. Characterization of the murine fatty acid transport protein gene and its insulin response sequence. *J. Biol. Chem.* **273:** 27420–27429.

34. Frohnert, B. I., T. Y. Hui, and D. A. Bernlohr. 1999. Identification of a functional peroxisome proliferator-responsive element in the murine fatty acid transport protein gene. *J. Biol. Chem.* **274:** 3970–3977.

35. Berk, P. D., S. L. Zhou, C. L. Kiang, D. Stump, M. Bradbury, and L. M. Isola. 1997. Uptake of long chain free fatty acids is selectively up-regulated in adipocytes of Zucker rats with genetic obesity and non-insulin-dependent diabetes mellitus. *J. Biol. Chem.* **272:** 8830–8835.

36. Coort, S. L., W. A. Coumans, A. Bonen, G. J. van der Vusse, J. F. Glatz, and J. J. Luiken. 2005. Divergent effects of rosiglitazone on

protein-mediated fatty acid uptake in adipose and in muscle tissues of Zucker rats. *J. Lipid Res.* **46:** 1295–1302.

37. Schaiff, W. T., I. Bildirici, M. Cheong, P. L. Chern, D. M. Nelson, and Y. Sadovsky. 2005. Peroxisome proliferator-activated receptor-gamma and retinoid X receptor signaling regulate fatty acid uptake by primary human placental trophoblasts. *J. Clin. Endocrinol. Metab.* **90:** 4267–4275.

38. Hauser, S., G. Adelmant, P. Sarraf, H. M. Wright, E. Mueller, and B. M. Spiegelman. 2000. Degradation of the peroxisome proliferator-activated receptor gamma is linked to ligand-dependent activation. *J. Biol. Chem.* **275:** 18527–18533.

39. Milger, K., T. Herrmann, C. Becker, D. Gotthardt, J. Zickwolf, R. Ehehalt, P. A. Watkins, W. Stremmel, and J. Fullekrug. 2006. Cellular uptake of fatty acids driven by the ER-localized acyl-CoA synthetase FATP4. *J. Cell Sci.* **119:** 4678–4688.

40. Reshef, L., Y. Olswang, H. Cassuto, B. Blum, C. M. Croniger, S. C. Kalhan, S. M. Tilghman, and R. W. Hanson. 2003. Glyceroneogenesis and the triglyceride/fatty acid cycle. *J. Biol. Chem.* **278:** 30413–30416.

41. Hellstrom, L., S. Reynisdottir, D. Langin, S. Rossner, and P. Arner. 1996. Regulation of lipolysis in fat cells of obese women during long-term hypocaloric diet. *Int. J. Obes. Relat. Metab. Disord.* **20:** 745–752.

42. Brasaemle, D. L., G. Dolios, L. Shapiro, and R. Wang. 2004. Proteomic analysis of proteins associated with lipid droplets of basal and lipolytically stimulated 3T3-L1 adipocytes. *J. Biol. Chem.* **279:** 46835–46842.

43. Stuhlsatz-Krouper, S. M., N. E. Bennett, and J. E. Schaffer. 1998. Substitution of alanine for serine 250 in the murine fatty acid transport protein inhibits long chain fatty acid transport. *J. Biol. Chem.* **273:** 28642–28650.

44. Ost, A., U. Ortegren, J. Gustavsson, F. H. Nystrom, and P. Stralfors. 2005. Triacylglycerol is synthesized in a specific subclass of caveolae in primary adipocytes. *J. Biol. Chem.* **280:** 5–8.

45. Wu, Q., A. M. Ortegon, B. Tsang, H. Doege, K. R. Feingold, and A. Stahl. 2006. FATP1 is an insulin-sensitive fatty acid transporter involved in diet-induced obesity. *Mol. Cell. Biol.* **26:** 3455–3467.

46. Chavez, J. A., and S. A. Summers. 2003. Characterizing the effects of saturated fatty acids on insulin signaling and ceramide and diacylglycerol accumulation in 3T3-L1 adipocytes and C2C12 myotubes. *Arch. Biochem. Biophys.* **419:** 101–109.